

See discussions, stats, and author profiles for this publication at: <https://www.researchgate.net/publication/317284528>

Quantum non-demolition measurement of single phonon state with nitrogen-vacancy centers ensemble and superconducting qubit

Article in Optics Express · May 2017

DOI: 10.1364/OE.25.030149

CITATION

1

READS

46

4 authors, including:



Zhang-qi Yin

Tsinghua University

67 PUBLICATIONS **1,277** CITATIONS

[SEE PROFILE](#)



Gui Lu Long

Tsinghua University

398 PUBLICATIONS **11,463** CITATIONS

[SEE PROFILE](#)

Some of the authors of this publication are also working on these related projects:



recommendation system [View project](#)



optically levitated nanoparticle [View project](#)

Quantum non-demolition measurement of single phonon state with nitrogen-vacancy centers ensemble and superconducting qubit

Rui-xia Wang,¹ Kang Cai,¹ Zhang-qi Yin,^{2,*} and Gui-lu Long^{1,†}

¹*Department of Physics, Tsinghua University, Beijing 100084, China*

²*Center for Quantum Information, Institute for Interdisciplinary Information Sciences, Tsinghua University, Beijing 100084, China*

(Dated: June 1, 2017)

We propose a scheme to realize the quantum non-demolition single phonon detection and emission based on the interaction between the NV ensemble and the superconducting flux qubit. The resonant frequency of the flux qubit will change with the NVE absorbing a single phonon, then we can detect the single phonon state through measuring the frequency shift of the flux qubit. The fidelity of the absorbing process can reach a much high value. After the detection process, the NVE can emit the absorbed phonon as we apply a driving pulse which is in reverse to the absorbing process. The overlap between the input and the output phonon shapes can reach 98.57%. The scheme can be realized under the realistic experimental condition.

PACS numbers: 63.20.kp, 63.20.dd, 03.67.Lx

I. INTRODUCTION

In quantum information processing, one of the key challenges is how to realize effective coupling, or communication, between distant qubits. Usually, the photons are used as flying qubits for quantum communications, or inducing effective coupling between distant qubits. For example, in superconducting quantum circuit systems, the microwave photon that is confined in transmission lines cavity is used as quantum bus. Recently, with the advances in the fabrication and manipulation of the mechanical systems[1–4], an alternative way of using phonon as quantum bus is widely studied [5]. The surface acoustic wave (SAW) was successfully coupled with superconducting qubits. The speed of SAW is 5 orders of magnitude slower than the speed of light [6, 7]. Therefore, the wavelength of SAW at GHz is also 5 orders of magnitude smaller than the microwave light. In this way, the single superconducting qubit addressing by SAW is possible. There are many schemes which have been proposed for researching and controlling the phonons, for example, the phonon preparation [8–10], detection [8–14], and realizing some functions by controlling and detecting the phonons [15, 16] in various systems. In order to further develop the phonon based quantum information processing, powerful and efficient phonon detectors are needed. The ultimate goal is to realize quantum non-demolition(QND) measurement on single phonon state. We proposed a scheme to realize the QND measurement of the phonon number states with the NV centers ensemble and the superconducting qubit.

The nitrogen-vacancy (NV) center, which consists a substitutional nitrogen atom and adjacent vacancy in diamond, is one of the most promising system for solid-

state quantum information processing. NV centers can be microwave controlled with long coherence time even at room temperature. The diamond lattice vibration will generate phonons, which can be tightly coupled with the NV center ensemble (NVE) [17, 18] and be cooled by the NVE [19]. However, the phonon number QND measurement hasn't been realized in the NVE system.

The hybrid system that the NVE couples to the superconducting flux qubit can in principle be used for phonon number detection and single phonon emission. The coupling strength between the NVE and the superconducting circuit can reach a strong regime [20–28]. In Ref. [?], in order to generate the entanglement between two NVEs, they coupled with a big superconducting gap-tunable flux qubit. In the hybrid system model, the frequency splitting between two of the NV center's energy levels has been adjusted to be equal to the resonant frequency of the flux qubit.

In this work, we revisit the model and modified some details as required which is shown in Fig. 1a. Here we include the coupling between the mechanical mode and the NVE. In order to reduce the disturbance to the phonon state, the superconducting flux qubit is suspended on the top of the diamond which are very close to but not in touch with each other. The energy levels in the NV centers can be adjusted by the magnetic field intensity which acts on the diamond according to our demands. The coupling strength between the NVE and superconducting flux qubit can be enhanced by a factor \sqrt{N} through the collective excitation, which can reach the strong coupling regime, as well as the coupling between the NVE and the single phonon. The single phonon can be absorbed by the NVE, which will induce the resonance frequency shift of the superconducting flux qubit. Then we can measure the single phonon state through probing the frequency shift of the superconducting flux qubit.

The inverse process of the single phonon detection is a emission process. The emitted phonon shape can be controlled by regulating the driving pulse acting on the

* yinzhangqi@tsinghua.edu.cn

† gllong@tsinghua.edu.cn

NVE. The similarity between the emitted and the absorbed single phonon can reach 98.57% if we inverse the driving pulse when emitting compared with the absorbing process. If the single phonon state is in quantum state before absorbing, the size and shape of the phonon will not be changed when emitting, this process is a quantum non-demolition (QND) measurement process, which realizes an ideal projective measurement that leaves the system in an eigenstate of the phonon number [30–33].

II. MODEL

As schematically shown in Fig. 1(a), we consider a diamond NVE fixed under a superconducting flux qubit which consists of four Josephson junctions. The flux qubit and NVE are coupled to each other for the detection of the state of the NVE, which are initially tuned to be uncoupled.

With a zero magnetic field, the spin-triplet ground state of the NV center splits into two energy levels, $M_s = 0$ and the nearly degenerate sublevels $M_s = \pm 1$ [34]. We apply an external magnetic field \vec{B}_{ext} along the crystalline direction [100] of the NV center [35] to split the degenerate sublevels $M_s = \pm 1$, which results in a three-level system denoted by $|0\rangle = |^3A, M_s = 0\rangle$, $|-1\rangle = |^3A, M_s = -1\rangle$, $|+1\rangle = |^3A, M_s = +1\rangle$, respectively. The schematic diagram of the NV center energy structure is shown in Fig. 1(b).

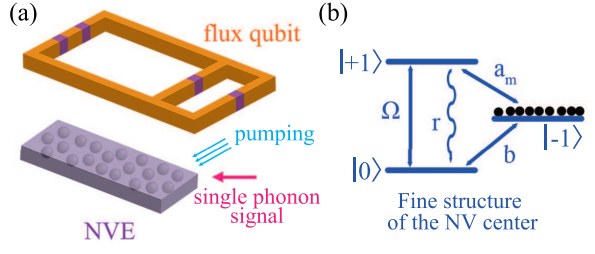


FIG. 1. (a) A schematic diagram of the phonon number detection system, which consists of a diamond NVE and a superconducting flux qubit. (b) The electron energy structure of the NV center electron spin. Ω is the Rabi frequency of the microwave drive. a_m is the phonon mode. b is the superconducting resonator mode. γ is the NVE decay rate.

The NV centers exist in a diamond crystal and they can sense the lattice vibrations. If there is a phonon produced in the lattice, the NV center can absorb it when the mechanical frequency and the energy splitting of the NV centers are matched [36, 37]. For this system, the phonon mode a_m with the frequency ω_m couples to the NV centers with transition of $|-1\rangle$ to $|+1\rangle$. A classical microwave field $\varepsilon(t) = \tilde{\varepsilon}(t)e^{-i\omega_0 t}$ drives the transition $|+1\rangle$ to $|0\rangle$ with a Rabi oscillation frequency $\Omega(t)$ (ω_0 is the frequency splitting between the levels $|0\rangle$ and $|+1\rangle$). The Rabi frequency $\Omega(t)$ can be written as $\Omega(t) =$

$\Omega_0\alpha(t)$. Within a good approximation, we assume that $\tilde{\varepsilon}(t)$ increase gradually from zero with $\tilde{\varepsilon}(0) \simeq 0$ to a finite strength. We have $\alpha(t) \propto \tilde{\varepsilon}(t)$, then we can get $\Omega(t) = \Omega'_0\tilde{\varepsilon}(t)$, which implies that the shape of the amplitude of the classical driving microwave field totally decide the Rabi frequency.

Neglecting the dissipation of the NVE system, the Hamiltonian of the NVE system including the coupling between the mode a_m and the output can be written as (setting $\hbar = 1$) [38, 39]

$$\begin{aligned}
 H = & \sum_{i=1}^N G_m (|+1\rangle_i \langle -1| a_m + |-1\rangle_i \langle +1| a_m^\dagger) \\
 & + \frac{\Omega_s(t)}{2} \sum_{i=1}^N (|0\rangle_i \langle +1| + |+1\rangle_i \langle 0|) \\
 & + i\sqrt{\kappa/2\pi} \int_{+\Delta\omega_e}^{+\Delta\omega_e} d\omega [a_m^\dagger e(\omega) - a_m e^\dagger(\omega)] \\
 & + \int_{+\Delta\omega_e}^{+\Delta\omega_e} d\omega [\omega e^\dagger(\omega) e(\omega)]. \quad (1)
 \end{aligned}$$

Where G_m is the coupling rate for single NV center and the phonon, which is typically small. $e(\omega)$ denotes the one-dimensional phonon modes which are free in the diamond and couple to the phonon mode a_m . We need to consider the free propagating modes within a finite bandwidth $[\omega_e - \Delta\omega_e, \omega_e + \Delta\omega_e]$ that couple to the NV mode with the carrier frequency ω_e . Within this bandwidth, the coupling between $e(\omega)$ and the NV is a constant approximately, and we denoted by $\sqrt{\kappa/2\pi}$ for convenience. κ is the effective decay rate.

To obtain the relationship between the driving pulse shape and the output phonon pulse shape, we first look at a simple picture by neglecting the dissipation of the NVE system and the coupling of the mode a_m to the output. Initially, we can cool the NVE to the ground state $|0\rangle$, and drive a π pulse between the state $|0\rangle$ and $|-1\rangle$ and then the NVE is in $|-1\rangle^{\otimes N}$. We assume that the phonon mode frequency ω_m equals to ω_e (ω_e is the frequency splitting between the levels $|-1\rangle$ and $|+1\rangle$). In the rotating frame, the Hamiltonian of the NVE system is

$$\begin{aligned}
 H' = & \sum_{i=1}^N G_m (|+1\rangle_i \langle -1| a_m + |-1\rangle_i \langle +1| a_m^\dagger) \\
 & + \frac{\Omega(t)_s}{2} \sum_{i=1}^N (|0\rangle_i \langle +1| + |+1\rangle_i \langle 0|). \quad (2)
 \end{aligned}$$

We map the operator $|+1\rangle_i \langle -1|$ to the bosonic operator. $\sqrt{N}a^\dagger = \sum_{i=1}^N |+1\rangle_i \langle -1|$, $a^\dagger a|n\rangle_{+1} = n|n\rangle_{+1}$ means there are n NVs that are in the state $|+1\rangle$, and then the Hamiltonian can be written as follow, where $g_m = \sqrt{N}G_m$.

We map the operators $|+1\rangle_i \langle -1|$ and $|0\rangle_i \langle +1|$ to the bosonic operators. $\sqrt{N}a^\dagger = \sum_{i=1}^N |+1\rangle_i \langle -1|$, $a^\dagger a|n\rangle_{+1} =$

$n|n\rangle_{+1}$ means there are n NVs that are in the state $|+1\rangle$, $\sqrt{N}d^\dagger = \sum_{i=1}^N |0\rangle_i \langle +1|$, $d^\dagger d|n\rangle_0 = n|n\rangle_0$ means there are n NVs that are in the state $|0\rangle$, and then the Hamiltonian can be written as follow, where $g_m = \sqrt{N}G_m$ and $\Omega(t) = \sqrt{N}\Omega_s(t)$.

$$H' = g_m(a^\dagger a_m + aa_m^\dagger) + \frac{\Omega(t)}{2}(d^\dagger + d). \quad (3)$$

In the bases of $|N\rangle_{-1}|0\rangle_{+1}|0\rangle_0|1\rangle_m$, $|N-1\rangle_{-1}|1\rangle_{+1}|0\rangle_0|0\rangle_m$, $|N-1\rangle_{-1}|0\rangle_{+1}|1\rangle_0|0\rangle_m$, where the state $|p\rangle_{-1}|q\rangle_{+1}|r\rangle_0|s\rangle_m$ represents that the numbers of the NVs which are in the states $|-1\rangle$, $|+1\rangle$, and $|0\rangle$ are p , q and r respectively, and the number of phonons in the diamond is s . The Hamiltonian can be written as a matrix as follow in the three bases,

$$H' = \begin{bmatrix} 0 & g_m & 0 \\ g_m & 0 & \frac{\Omega(t)}{2} \\ 0 & \frac{\Omega(t)}{2} & 0 \end{bmatrix}. \quad (4)$$

This Hamiltonian has the well-known dark state $|D\rangle$ with the form $|D\rangle = \frac{-\Omega(t)/2}{\sqrt{g_m^2 + [\Omega(t)/2]^2}} |N\rangle_{-1}|0\rangle_{+1}|0\rangle_0|1\rangle_m + \frac{g_m}{\sqrt{g_m^2 + [\Omega(t)/2]^2}} |N-1\rangle_{-1}|0\rangle_{+1}|1\rangle_0|0\rangle_m$. The dark state means, the state will remain on the state $|D\rangle$, if the driving pulse $\Omega(t)$ and the coupling strength satisfy the relationship $\cos\theta = \frac{\Omega(t)/2}{\sqrt{g_m^2 + [\Omega(t)/2]^2}}$ and $\sin\theta = \frac{g_m}{\sqrt{g_m^2 + [\Omega(t)/2]^2}}$.

We analyze the effects of non-zero dissipation in section IV when calculating the phonon detecting efficiency and the overlap of the absorbing and emitting a single phonon with the real lossy system.

III. INTERACTION BETWEEN THE NVE AND THE PHONON

To obtain the relationship of the pulse shape between the driving and the phonon, we first consider the emitting process from state $|N-1\rangle_{-1}|0\rangle_{+1}|1\rangle_0|0\rangle_m$ to $|N\rangle_{-1}|0\rangle_{+1}|0\rangle_0|1\rangle_m$ under idea conditions. The Hamiltonian of the system can be written as

$$\begin{aligned} H &= g_m(a^\dagger a_m + aa_m^\dagger) + \frac{\Omega(t)}{2}(d^\dagger + d) \\ &+ i\sqrt{\kappa/2\pi} \int_{-\Delta\omega_e}^{+\Delta\omega_e} d\omega [a_m^\dagger e(\omega) - a_m e^\dagger(\omega)] \\ &+ \int_{-\Delta\omega_e}^{+\Delta\omega_e} d\omega [\omega e^\dagger(\omega) e(\omega)]. \end{aligned} \quad (5)$$

Assume that, at the time $t = 0$, the Rabi frequency $\Omega(t) = 0$, the NVE system are in the state $|N-1\rangle_{-1}|0\rangle_{+1}|1\rangle_0|0\rangle_m$, after applying a classical driving pulse $\varepsilon(t)$, the Rabi frequency, which is proportional

to the intensity of the driving pulse, changes slowly and is within the adiabatic approximation. Then we can expand the state $|\Psi\rangle$ of the whole system into the following form [38]

$$|\Psi\rangle = c_d|D\rangle \otimes |\phi_0\rangle + |N\rangle_{-1}|0\rangle_{+1}|0\rangle_0|0\rangle_m \otimes |\phi_1\rangle, \quad (6)$$

where $|\phi_0\rangle$ denotes the vacuum state of mode $e(\omega)$ in the diamond, and

$$|\phi_1\rangle = \int_{-\Delta\omega_e}^{+\Delta\omega_e} d\omega c_\omega e^\dagger(\omega) |\phi_0\rangle, \quad (7)$$

represents the single phonon output state. Initially, $c_d = 1$, $c_\omega = 0$ and $\Omega(0) = 0$. Within the adiabatic approximation, we would like to calculate the time evolution of the whole NVE system state $|\Psi\rangle$ by substituting it into the schrodinger equation $i\partial_t|\Psi\rangle = H|\Psi\rangle$. The coefficients c_d and c_ω can get, which satisfy the following evolution equations:

$$\dot{c}_d = \left(-\sqrt{\kappa/2\pi} \cos\theta\right) \int_{-\Delta\omega_e}^{+\Delta\omega_e} c_\omega d\omega, \quad (8)$$

$$\dot{c}_\omega = -i\omega c_\omega + \sqrt{\kappa/2\pi} c_d \cos\theta. \quad (9)$$

We can get the solution of c_ω as follow

$$c_\omega(t) = \sqrt{\kappa/2\pi} \int_0^t e^{-i\omega(t-\tau)} c_d(\tau) \cos\theta(\tau) d\tau, \quad (10)$$

substituting the solution into the equation of c_d , leads to

$$\dot{c}_d = -\frac{\kappa \cos\theta}{\pi} \int_0^t \frac{\sin[\delta\omega(t-\tau)]}{(t-\tau)} c_d(\tau) \cos\theta(\tau) d\tau \quad (11)$$

The bandwidth $\delta\omega$ satisfies $\delta\omega T \gg 1$, where the operation time T characterizes the time scale for a significant change of c_d and $\sin\theta$, so the above function satisfies a δ function

$$\delta(x) = \lim_{k \rightarrow \infty} \frac{1}{\pi} \frac{\sin kx}{x}, \quad (12)$$

then we can obtain

$$\dot{c}_d = -\frac{\kappa}{2} c_d(t) \cos^2\theta, \quad (13)$$

The solution of c_d and c_ω are

$$c_d = e^{-\frac{\kappa}{2} \int_0^t \cos^2\theta(\tau) d\tau}, \quad (14)$$

$$\begin{aligned} c_\omega(t) &= \sqrt{\kappa/2\pi} \int_0^t e^{-i\omega(t-\tau)} e^{-\frac{\kappa}{2} \int_0^t \cos^2\theta(\tau) d\tau} \\ &\cdot \cos\theta(\tau) d\tau. \end{aligned} \quad (15)$$

The single-phonon pulse shape $f(t)$ can be obtained by the Fourier transformation

$$f(t) = \frac{1}{\sqrt{2\pi}} \int_{-\Delta\omega_e}^{+\Delta\omega_e} d\omega c_\omega(T) e^{-i\omega(t-T)} \quad (16)$$

$$= \sqrt{\kappa} \cos\theta(t) e^{-\frac{\kappa}{2} \int_0^t \cos^2\theta(\tau) d\tau}. \quad (17)$$

If the Rabi frequency $\Omega(t)$, which is proportional to the strength of the driving pulse, satisfies the function as $\Omega(t) = 2g_m \exp[\kappa(t - \frac{T}{2})/2]$, the output phonon shape will be symmetric. We can figure out the output phonon shape function as

$$f(t) = \frac{\sqrt{\kappa} \sqrt{1 + \exp(-\frac{\kappa T}{2})}}{\exp[-\kappa(t - \frac{T}{2})/2] + \exp[\kappa(t - \frac{T}{2})/2]}, \quad (18)$$

the results is shown in Fig. 3 for $\kappa/2\pi = 1.6 \times 10^5$, $T = \frac{20}{\kappa}$. We assume that, in the absorption process, we know the phonon shape in advance, such as the shape in Fig. 2. As the absorption process is the time reversal of the emission process, and the phonon shape is symmetrical in the time domain, if we reverse the temporal driving pulse shape on NV centers in the absorbing process, the phonon can be completely absorbed by the NVE [40]. If the phonon shape is not symmetrical in the time domain, it can also be completely absorbed as long as it is reversed simultaneously with the driving pulse.

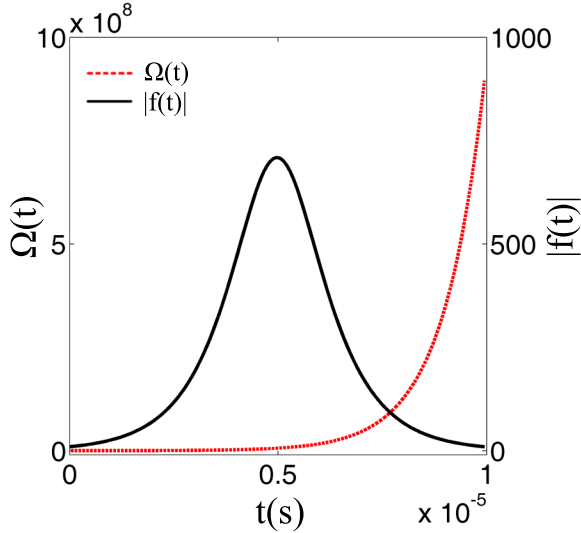


FIG. 2. The situation of the symmetric output phonon shape. The red line is the driving pulse shape applying to the NVE, and the black line represents the pulse shape of the output phonon.

IV. QND SINGLE PHONON STATE DETECTION

As schematically shown in Fig. 1, we consider a diamond NVE couples to a superconducting flux qubit, which consists of four Josephson junctions. The gap frequency of the flux qubit can be tuned by the magnetic field applied to it [29]. So we can tune the gap frequency to be equal to ω_c , which is the NV center frequency splitting between the levels $|0\rangle$ and $|-1\rangle$. Using the Holstein-Primakoff (HP) transformation and mapping the operators to the bosonic operators as follows: $\sqrt{N}b^\dagger = \sum_{i=1}^N |0\rangle_i \langle -1|$, where the operators b and b^\dagger obey the standard bosonic commutator $[b, b^\dagger] = 1$. We assume that, initially, the NV centers are all in the state $|-1\rangle$, after absorbing the phonons, there are a small quantity of NV centers being in the state $|0\rangle$, the number of which is far less than the total number N .

Regulating the splitting frequency of the flux qubit and the driving pulse frequency, in the rotating frame, we can get the interaction Hamiltonian of the coupling system as follows [29]

$$H_I = \sqrt{\frac{N}{2}} g (b^\dagger \sigma_- + b \sigma_+). \quad (19)$$

Where N is the total number of the NV centers contained in the NVE, $\sigma_\pm = \frac{1}{2}(\sigma_x \pm i\sigma_y)$, σ_x and σ_y are usual Pauli operators in the basis of flux eigenstate which stand for the clockwise and counterclockwise persistent current. $\langle b^\dagger b \rangle \ll N$ means the number of the NV centers which are in the state $|0\rangle$ after absorbing phonons is far less than the total number of NVE which are in the state $|-1\rangle$. g is the effective coupling strength between the NVE and the flux qubit which depends on the Bohr magneton, the ground state Landé factor of the NVE and the magnetic field produced by the flux qubit.

Then, we may add a detuning Δ in this transition, where $H_0 = \Delta b^\dagger b$. The total Hamiltonian $H_{tot} = H_0 + H'_I$, the effective Hamiltonian is

$$H_{tot} = \Delta b^\dagger b + \sqrt{\frac{N}{2}} g (b^\dagger \sigma_- + b \sigma_+), \quad (20)$$

in the rotating wave approximation, the Hamiltonian becomes

$$H_r = \sqrt{\frac{N}{2}} g (b^\dagger \sigma_- e^{i\Delta t} + b \sigma_+ e^{-i\Delta t}). \quad (21)$$

When the interaction strength of $\sqrt{\frac{N}{2}}g$ is far small compared with the detuning Δ , we can calculate the time-averaged effective Hamiltonian as [41] $H_{eff} = -\frac{Ng^2}{2\Delta} b^\dagger b \sigma_z - \frac{Ng^2}{2\Delta} \sigma_+ \sigma_-$. From the Hamiltonian we can see that the resonant frequency of the flux qubit will be

affected by the states of NVE, which means frequency shift is proportional to the excitation number in state $|0\rangle$. If there are n NV centers absorbing n phonons and jumping from state $|-1\rangle$ to state $|0\rangle$, the frequency shift of the flux qubit is $f_s = -\frac{Ng^2}{2\Delta}n$. When the value of $b^\dagger b$ changes from n to m , the frequency shift changes by $\Delta f_s = \frac{Ng^2}{2\Delta}(n-m)$, where $|n-m| \geq 1$. After absorbing the phonons, we can measure the frequency shift of the superconducting flux qubit, and then, give a driving pulse which is inverse to the absorbing process in time domain, the phonons will be emitted. Since the absorbing processes are reversible, and the emitting process here is the inverse process, ideally, the emitting phonons have the same waveform with the input ones in case of the input phonons are single phonon or in Fock state. This measurement is a QND measurement.

When $|n-m| = 1$, which is the minimum shift in the measurement process, the change of the frequency shift takes the minimum possible value as

$$\Delta f_s = \frac{Ng^2}{2\Delta}. \quad (22)$$

We set $g = 2\pi \times 2kHz$, $N = 8 \times 10^4$, $\Delta = 2\pi \times 4MHz$, which is within the reach of the experiment feasibility [42], the frequency shift $\Delta f_s = \frac{Ng^2}{2\Delta} = 2\pi \times 40kHz \doteq 251kHz$. If the frequency shift is much sharper than the line width of σ_z mode, we can resolve it clearly. Current designs has reached that the line width of σ_z mode is less than $25kHz$ [43]. Therefore, in principle, the single excitation from state $|-1\rangle$ to state $|0\rangle$ can be detected distinctly.

V. EFFICIENCY WITH SYSTEM DISSIPATION

We have analysed the dynamical evolution and got the relationship between the driving pulse shape and the emitting phonon shape in ideal condition, however, there are various losses in the real systems. If we consider the dynamical evolution of the NVE system with the conditional Hamiltonian which include the possible losses, the whole conditional Hamiltonian has following form:

$$\begin{aligned} H_c = & -i\frac{\gamma_1}{2}|N-1\rangle_{-1}|1\rangle_{+1}|0\rangle_0|0\rangle_m \\ & -i\frac{\gamma_0}{2}|N-1\rangle_{-1}|0\rangle_{+1}|1\rangle_0|0\rangle_m - i\frac{\gamma_m}{2}a_m^\dagger a_m \\ & + g_m(a_m^\dagger a_m + aa_m^\dagger) + \frac{\Omega(t)}{2}(d^\dagger + d) \\ & + i\sqrt{\kappa/2\pi} \int_{-\Delta\omega_e}^{+\Delta\omega_e} d\omega [a_m^\dagger e(\omega) - a_m e^\dagger(\omega)] \\ & + \int_{-\Delta\omega_e}^{+\Delta\omega_e} d\omega [\omega e^\dagger(\omega) e(\omega)]. \end{aligned} \quad (23)$$

Where γ_0 is the dephasing rate in state $|0\rangle$, γ_1 denotes the spontaneous emission of state $|+1\rangle$, and γ_m denotes the phonon dissipation in the single NV evolution.

For numerical simulations, we need to discretize the field $e(\omega)$ by introducing a finite but small frequency interval $\delta\omega$ between two adjacent mode frequency. Then the number of the total modes we have is $n = \frac{2\Delta\omega_e}{\delta\omega} + 1$, the frequency of the j th mode ω_j which is denoted by e_j is given by $\omega_j = (j - \frac{n+1}{2})\delta\omega$. The Hamiltonian can be transformed to the form:

$$\begin{aligned} H_c = & -i\frac{\gamma_1}{2}|N-1\rangle_{-1}|1\rangle_{+1}|0\rangle_0|0\rangle_m \\ & -i\frac{\gamma_0}{2}|N-1\rangle_{-1}|0\rangle_{+1}|1\rangle_0|0\rangle_m - i\frac{\gamma_m}{2}a_m^\dagger a_m \\ & + g_m(a_m^\dagger a_m + aa_m^\dagger) + \frac{\Omega(t)}{2}(d^\dagger + d) \\ & + i\kappa_e \sum_{j=1}^n \sqrt{\delta\omega} [a_m^\dagger e_j - a_m e_j^\dagger] \\ & + \sum_{j=1}^n (\omega_j \delta\omega e_j^\dagger e_j), \end{aligned} \quad (24)$$

where $\kappa_e = \sqrt{\kappa\delta\omega/2\pi}$. Similarly, we can expand the state $|\Psi\rangle$ of the NVE system with the phonon pulse state replace by $|\phi_1\rangle = \sum_{j=1}^n \delta\omega b_j e_j^\dagger |vac\rangle$, which is

$$\begin{aligned} |\Psi\rangle = & (c_1|N-1\rangle_{-1}|0\rangle_{+1}|0\rangle_0|1\rangle_m + c_2|N-1\rangle_{-1}|1\rangle_{+1}|0\rangle_0|0\rangle_m \\ & + c_3|N-1\rangle_{-1}|0\rangle_{+1}|1\rangle_0|0\rangle_m) \otimes |\phi_0\rangle \\ & + |N-1\rangle_{-1}|0\rangle_{+1}|0\rangle_0|0\rangle_m \otimes |\phi_1\rangle. \end{aligned} \quad (25)$$

Substituting $|\Psi\rangle$ into the schrodinger equation $i\partial_t|\Psi\rangle = H|\Psi\rangle$, we can get

$$\dot{c}_1 = -\frac{\gamma_m}{2}c_1 - ig_m c_2 + \kappa_e \sum_{j=1}^n \tilde{b}_j, \quad (26)$$

$$\dot{c}_2 = -\frac{\gamma_1}{2}c_2 - ig_m c_1 - i\frac{\Omega(t)}{2}c_3, \quad (27)$$

$$\dot{c}_3 = -\frac{\gamma_0}{2}c_3 - i\frac{\Omega(t)}{2}c_2, \quad (28)$$

$$\dot{b}_j = -\kappa_e c_1 - i\tilde{b}_j \omega_j, \quad (29)$$

where $\tilde{b}_j = \sqrt{\delta\omega} b_j$. We assume that, initially, there is a single phonon state in the diamond, which shape is shown as Fig. 2, and all of the NV centers are in the state $|-1\rangle$, which means $c_1 = c_2 = c_3 = 0$, $\sum |b_j|^2 \neq 0$. If we would like to absorb the phonon effectively, the driving pulse $\Omega'(t)$ should be the time reversal of $\Omega(t)$ in Fig. 2, which is $\Omega'(t) = g_m \exp[\kappa(-t + \frac{T}{2})/2]$, where $T = 20/\kappa$. The shape control of the driving microwave pulse can be easily achieved by modulating an arbitrary wave generator. We set $\gamma_0/2\pi = 0.16kHz$, $\gamma_1/2\pi = 0.16kHz$ [44], $\gamma_m/2\pi = 0.16kHz$ [17, 45], $g_m/2\pi = 0.96MHz$, and $\kappa/2\pi = 0.32MHz$. The numerical simulation results

of absorbing process is shown in Fig. 3a with the black lines. Under the condition of strong coupling between the NVE and the phonon, the process is quasi-adiabatic, the value of c_2 is distinctly smaller than c_1 and c_3 . The first half is the process that the free single phonon entering the strong coupling area with the NVE plays a leading role, and the later half is predominantly the absorbing process. at time $t = T$, the fidelity between the actual state and the ideal state is 99.38%. As the dissipations increase, the fidelity decreases obviously which is also shown in Fig. 3a with the blue lines. The red lines in Fig. 3a implies that, it will also reduce the fidelity of the state if the coupling strength and the effective decay rate κ do not satisfy the adiabatic condition.

After absorbing the single phonon, we can apply a driving pulse $\Omega(t)$ on the NVE, the phonon we have just absorbed will then be emitted. The comparison of the input and output phonon pulse shape is shown in Fig. 3b with the $\kappa = 0.32MHz$. The black line is the input phonon shape, the red, blue and green ones are the output phonon shape with $g_m/2\pi = 0.96MHz$, $0.64MHz$ and $0.32MHz$ respectively. we can see that, the more stronger the coupling is, the more overlap it has between the input and output single phonon shape. When the coupling strength $g_m/2\pi = 0.96MHz$, the overlap can reach 98.57%. In the first step, the NVE absorbs one phonon from the diamond or not. And then, we can detecting whether the single phonon state was absorbed through the frequency shift of the coupled superconducting flux qubit. Finally, the NVE can emit the phonon with nearly the same shape compared with the absorbed one. In this process, the single phonon state has been measured without changing the phonon shape, which is a true QND measurement. The process of emitting can act as a single phonon source. The whole courses including absorbing, detecting and emitting a single phonon can also serve as a single phonon memory.

VI. CONCLUSION

We have proposed a scheme to realize the QND single phonon state detecting and emitting based on the interaction between the NVE and the superconducting flux qubit. By analyze the dynamical evolution of the real system, we are able to calculate the fidelity of the absorbing process and the overlap between the input and output phonon number state, both of which can reach a very high value. The emitting process can act as a single phonon source and the whole courses including absorbing, detecting and emitting a single phonon can also serve as a single phonon memory. In future, the similar method may also be used to realize the QND measurement for arbitrary Fock states of phonons.

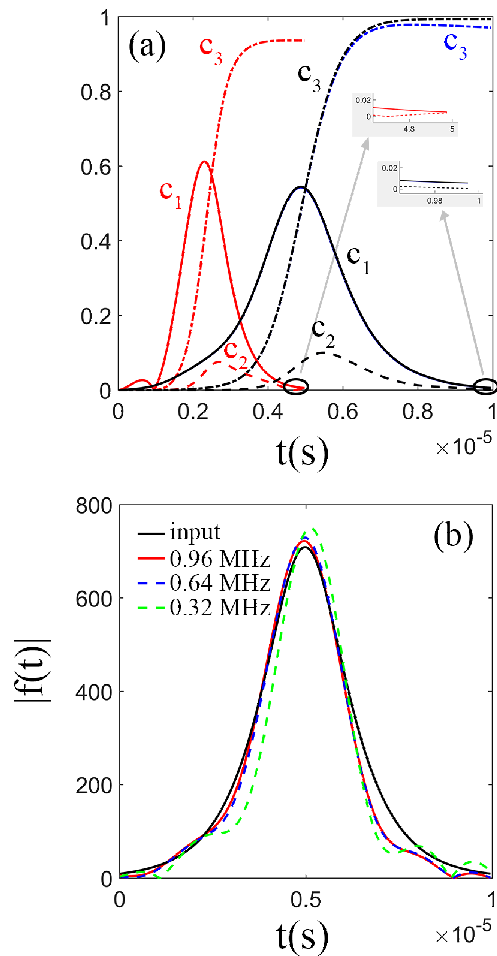


FIG. 3. The numerical simulation results. (a) is the absorbing process. The black lines represents the process with $\gamma_0/2\pi = 0.16kHz$, $\gamma_1/2\pi = 0.16kHz$, $\gamma_m/2\pi = 0.16kHz$, $g_m/2\pi = 0.96MHz$, and $\kappa/2\pi = 0.32MHz$. The blue lines show the process with $\gamma_0/2\pi = 1.6kHz$, $\gamma_1/2\pi = 1.6kHz$, $\gamma_m/2\pi = 1.6kHz$, $g_m/2\pi = 0.96MHz$, and $\kappa/2\pi = 0.32MHz$. The red ones denote the process with $\gamma_0/2\pi = 0.16kHz$, $\gamma_m/2\pi = 0.16kHz$, $g_m/2\pi = 1.92MHz$, and $\kappa/2\pi = 0.64MHz$. (b) is the emitting process, where the black line represents the input phonon shape, and the red, blue and green lines represent the output phonon shapes when the coupling strength are at $g_m/2\pi = 0.96MHz$, $0.64MHz$ and $0.32MHz$ respectively with the same value of $\kappa = 0.32MHz$. The overlap between the input pulse and the output pulse are 98.57%, 98.32% and 94.38% for the red, blue and green lines respectively.

ACKNOWLEDGMENTS

R.X.W. is supported by China Postdoctoral Science Foundation (2016M600999). Z.Q.Y. is supported by National Natural Science Foundation of China (NSFC) (61435007), and Joint Fund of the Ministry of Education of the Peoples Republic of China (MOE)

(6141A02011604). G.L.L is supported by National Natural Science Foundation of China (NSFC) (20141300566).

-
- [1] Q. Hou, W. Yang, C. Chen and Z. Yin, *J. Opt. Soc. Am. B* **33**, 2242 (2016).
- [2] X. Wang, A. Miranowicz, H. R. Li, F. Nori, *Phys. Rev. A* **93**, 063861 (2016).
- [3] , V. Stojanovic, E. Demler, M.Vanevic, and L. Tian, *Phys. Rev. B* **89**, 1098 (2014).
- [4] A. D. O’Connell, M. Hofheinz, M. Ansmann, et al., *Nature*, **464**, 7289 (2010).
- [5] M. J. A. Schuetz, E. M. Kessler, G. Giedke, L. M. K. Vandersypen, M. D. Lukin, and J. I. Cirac, *Phys. Rev. X* **5**, 031031 (2015).
- [6] R. Manenti, A. F. Kockum, A. Patterson, T. Behrle, J. Rahamim, G. Tancredi, F. Nori, and P. J. Leek, arXiv: 1703.04495v1 (2017).
- [7] M. V. Gustafsson, T. Aref, A. F. Kockum, M. K. Ekström, G. Johansson, and P. Delsing, *Science* **346**, 6206 (2014).
- [8] C. Galland, N. Sangouard, N. Piro, N. Gisin, and T. J. Kippenberg, *Phys. Rev. Lett.* **112**, 143602 (2014).
- [9] O. Matsuda and O. B. Wright, *Phys. Rev. B* **77**, 224110 (2008).
- [10] O. Matsuda, O. B. Wright, D. H. Hurley, V. E. Gusev, and K. Shimizu, *Phys. Rev. Lett.* **93**, 9 (2004).
- [11] Y. Yanay and A. A. Clerk, *New J. Phys.* **19**, 033014 (2017).
- [12] J. H. Chai, Y. Q. Lu, *Physica B* **291**, 292 (2000).
- [13] X. Baia, T. A. Eckhausea, S. Chakrabartib, P. Bhattacharyab, R. Merlina, C. Kurdak, *Physica E* **34**, 592 (2006).
- [14] M. J. Woolley, A. C. Doherty, and G. J. Milburn, *Phys. Rev. B* **82**, 094511 (2010).
- [15] C. Ohm, C. Stampfer, J. Splettstoesser, and M. R. Wegewijs, *Appl. Phys. Lett.* **100**, 143103 (2012).
- [16] O. P. Neto, M. C. Oliveira, F. Nicacio, and G. J. Milburn, *Phys. Rev. A* **90**, 023843 (2014).
- [17] P. Ovarthaiyapong, K. W. Lee, B. A. Myers, and A. C. B. Jayich, *Nat. Comm.* **5**, 4429 (2014).
- [18] D. A. Golter, T. Oo, M. Amezcuca, K. A. Stewart, and H. Wang, *Phys. Rev. Lett.* **116**, 143602 (2016).
- [19] E. R. MacQuarrie, M. Otten, S. K. Gray, and G. D. Fuchs, *Nat. Comm.* **8**, 14358 (2017)
- [20] Z. L. Xiang, S. Ashhab, J. Q. You, and F. Nori, *Rev. Mod. Phys.* **85**, 623 (2013).
- [21] Z. L. Xiang, X. Y. Lu, T. F. Li, J. Q. You, and F. Nori, *Phys. Rev. B* **87**, 144516 (2013).
- [22] Y. Kubo, et al., *Phys. Rev. Lett.* **105**, 140502 (2010).
- [23] D. I. Schuster, et al., *Phys. Rev. Lett.* **105**, 140501 (2010).
- [24] R. Amsüss, et al., *Phys. Rev. Lett.* **107**, 060502 (2011).
- [25] Y. Kubo, et al., *Phys. Rev. Lett.* **107**, 220501 (2011).
- [26] Y. Kubo, et al., *Phys. Rev. A* **85**, 012333 (2012).
- [27] X. Zhu, et al., *Nature* **478**, 221 (2011).
- [28] D. Marcos, et al., *Phys. Rev. Lett.* **105**, 210501 (2010).
- [29] W. L. Song, Z. q. Yin, W. L. Yang, X. B. Zhu, F. Zhou and M. Feng D. Marcos, et al., *Sci. Rep.* **5**, 7755 (2015).
- [30] S. Gleyzes, S. Kuhr, C. Guerlin, J. Bernu, S. Deléglise, U. B. Hoff, M. Brune, J. M. Raimond and S. Haroche, *Nature* **446**, 05589 (2007)
- [31] V. B. Braginsky, and F. Y. Khalili, *Quantum Measurement* (ed. Thorne, K. S.) Chs IV and XI (Cambridge Univ. Press, Cambridge, UK, 1992).
- [32] P. Grangier, J. A. Levenson, and J. P. Poizat, *Nature* **396**, 537 (1998).
- [33] G. Nogues, et al., *Nature* **400**, 239 (1999).
- [34] N. B. Manson, J. P. Harrison, and M. J. Sellars, *Phys. Rev. B* **74**, 104303 (2006).
- [35] S. Saito, X. Zhu, R. Amsüss, Y. Matsuzaki, K. Kakuyanagi, T. Shimo-Oka, N. Mizuochi, K. Nemoto, W. J. Munro, and K. Semba, *Phys. Rev. Lett.* **101**, 107008 (2013).
- [36] S. D. Bennett, N. Y. Yao, J. Otterbach, P. Zoller, P. Rabl, and M. D. Lukin, *Phys. Rev. Lett.* **110**, 156402 (2013).
- [37] Zhang-qi Yin, Zhao Nan, Tongcang Li, *Science China Physics, Mechanics & Astronomy* **58**, 050303 (2015),
- [38] L. M. Duan, A. Kuzmich, and H. J. Kimble, *Phys. Rev. A* **67**, 032305 (2003).
- [39] Zhang-qi Yin, W. L. Yang, Luyan Sun, L. M. Duan *Phys. Rev. A* **91**, 012333 (2015).
- [40] J. I. Cirac, P. Zoller, H. J. Kimble, and H. Mabuchi, *Phys. Rev. Lett.* **78**, 16 (1997).
- [41] D. F. V. James and J., *Canadian Journal of Physics*, **6**, 625 (2007).
- [42] X. Zhu, S. Saito, A. Kemp, et al., *Nature*, **478**, 221 (2011).
- [43] F. Yan , S. Gustavsson , A. Kamal , et al., *Nat. Commun.* **7**, 12964 (2016).
- [44] N. Bar-Gill, L.M. Pham, A. Jarmola, D. Budker, and R.L. Walsworth, *Nat. Commun.* **4**, 1743 (2013).
- [45] Y. Tao, J. M. Boss, B. A. Moores, and C. L. Degen, *Nat. Commun.* **5**, 3638 (2014).